JOURNAL OF NATURAL PRODUCTS

Article

pubs.acs.org/jnp

# Enantiomeric Derivatives of Tokinolide B: Absolute Configuration and Biological Properties

Alejandra León,[†] J. Antonio Cogordán,[†] Olov Sterner,[‡] and Guillermo Delgado*,[†]

[†]Instituto de Química de la Universidad Nacional Autónoma de México, Circuito Exterior, Ciudad Universitaria, Coyoacán 04510, México, D.F.

[‡]Division of Organic Chemistry, Lund University, P.O. Box 124, SE-22100 Lund, Sweden

Supporting Information

**ABSTRACT:** The enantiomeric lactams (−)-**8**, (+)-**8**, (+)-**9**, and (−)-**9** were formed by the reaction of the dimeric phthalide *rac*-tokinolide B (*rac*-**3**) with (*R*)-(+)-α-methylbenzylamine and (*S*)-(−)-α-methylbenzylamine. The absolute configurations of compounds **8** and **9** were assigned by experimental and theoretically calculated electronic circular dichroism methods for (+)-**8** and (−)-**9**. Compounds **3**, **5**, (−)-**8**, (+)-**8**, (+)-**9**, and (−)-**9** displayed cytotoxic activity toward several human tumor cell lines, with (−)-**8** and (−)-**9** being the most potent.

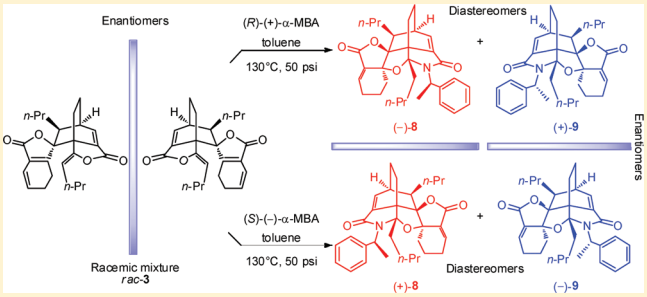


Natural phthalides are found in plants of the Umbelliferae family. The monomeric (*Z*)-ligustilide (**1**) and (*Z*)-butylidenephthalide (**2**), as well as the dimeric tokinolide B (**3**), diligustilide (**4**), and riligustilide (**5**), have been isolated from *Ligusticum porteri*,[1] the dimers being racemic mixtures **1**−**4** formed from **1** via $[_4\pi_s + _2\pi_s]$ and $[_2\pi_s + _2\pi_s]$ cycloadditions.[2,3] These natural phthalides are interesting for their chemical behavior such as the photochemical reaction of **1** to give **5**,[4] the relay synthesis of **3**−**5**,[5,6] and the formation of linear dimers from **1**.[7] Addition of methyl thioglycolate and benzylamine to (*Z*)-ligustilide (**1**) has established the electrophilic character of this monomer.[8] Under basic conditions **3** produced the pentacyclic compound cyclotokinolide B,[9] whereas base-catalyzed treatment of **4** afforded products from intramolecular reactions.[3] In Northern Mexico, the rhizomes of *L. porteri* are used by the Raramuri community for treating gastrointestinal disorders and for ritual curing ceremonies.[10,11] (*Z*)-Ligustilide (**1**) and (*Z*)-butylidenephthalide (**2**) exhibit several bioactivities, e.g., antiplatelet aggregation, antithrombosis, cardiac function modulation, and smooth muscle relaxation.[12−14] The biological activities of dimeric phthalides have been well recognized.[15,16] Considering the particular chemistry of the dimeric phthalides as well as their pharmacological activities, including the cytotoxic activities toward human cancer cell lines reported here, we were interested in preparing enantiomeric derivatives of *rac*-tokinolide B (*rac*-**3**) of known configuration that could be evaluated as cytotoxic agents.

## RESULTS AND DISCUSSION

Bearing in mind that *rac*-**3** possesses different electrophilic sites of varying reactivity, i.e., the carbonyl carbon as a hard acid via 1,2-addition and the β position of an α,β-unsaturated lactone as softer acid, it was envisaged that treatment with an enantiomerically pure amine such as (*R*)-(+)-α-methylbenzylamine would afford a pair of diastereomeric addition products [(−)-**8** + (+)-**9**] that could be separated by conventional methods. Treatment of *rac*-**3** with (*S*)-(−)-α-methylbenzylamine would produce another pair of diastereomers [(+)-**8** + (−)-**9**]. The expected stereochemical relationships between the two pairs of products are shown in Scheme 1. The absolute configuration of the products could be determined by the application of chiroptical and theoretical methods, as previously reported for several natural compounds.[17]

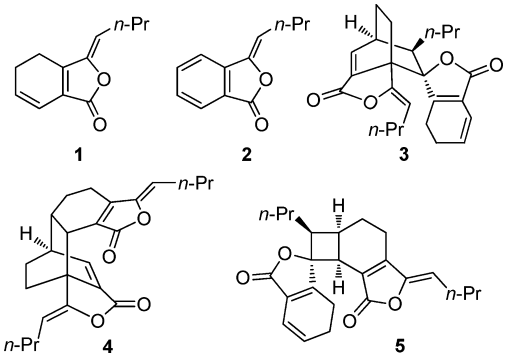


**Figure 1.** Representative monomeric and dimeric phthalides from *Ligusticum porteri*.

Treatment of *rac*-**3** in toluene under pressure (50 psi) with (*R*)-(+)-α-methylbenzylamine afforded a pair of diastereomeric compounds, (−)-**8** and (+)-**9**, as major and minor products, respectively. As anticipated, when (*S*)-(−)-α-methylbenzylamine was used as nucleophile under the same conditions,

**Received:** August 2, 2011
**Published:** May 10, 2012

**Scheme 1. Stereochemical Relationships of (−)-8, (+)-8, (+)-9, and (−)-9**

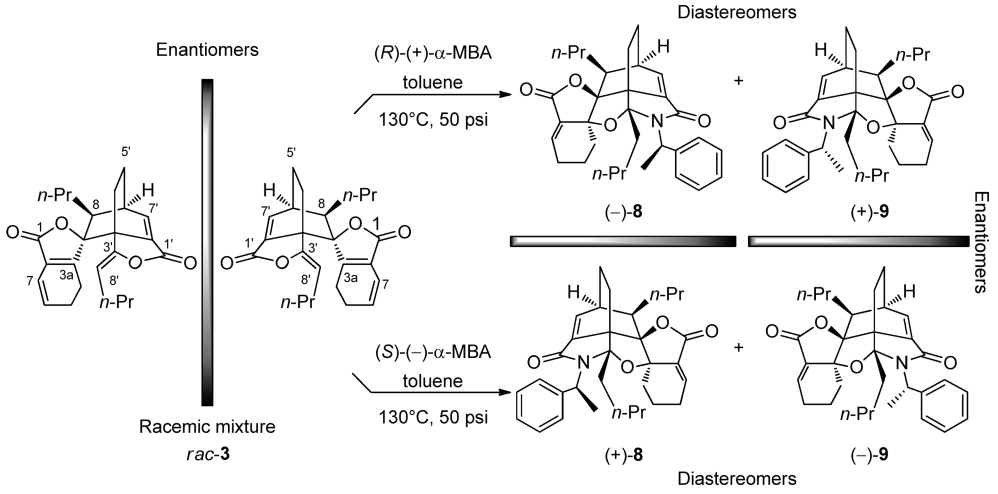


**Scheme 2. Proposed Mechanism for the Formation of (−)-8 and (+)-9 from *rac*-3**

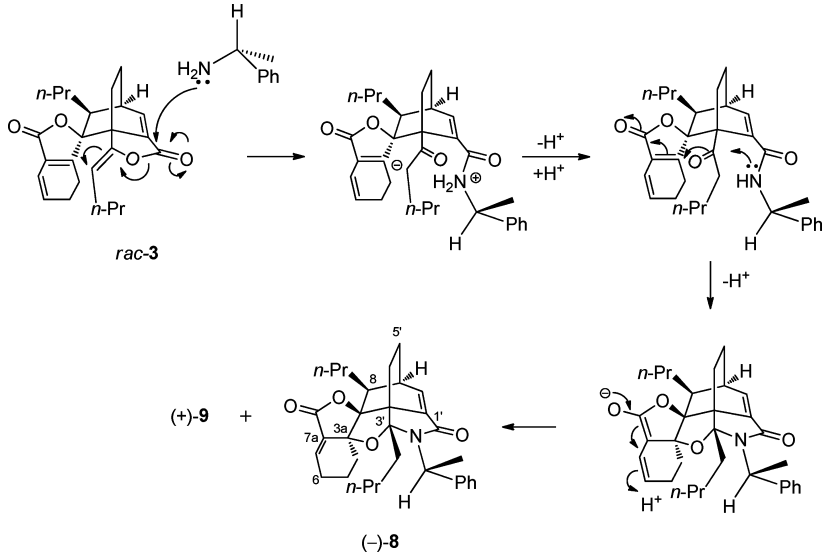


(+)-**8** and (−)-**9** were obtained as minor and major products, respectively. These stereochemical relationships were confirmed by the identity of the spectroscopic properties of (−)-**8** and (+)-**8**, and those of (+)-**9** and (−)-**9**, by the specific rotations and CD curves (see below and Experimental Section).

The products (−)-**8**, (+)-**8**, (+)-**9**, and (−)-**9** (Scheme 1) were stereoisomeric ($C_{32}H_{39}O_4N$) and derived from the addition of the amine ($C_8H_{11}N$) to the starting material ($C_{24}H_{28}O_4$), according to their molecular formulas established by FAB-HR-MS. The presence of (a) a $\gamma$-lactam conjugated with an endocyclic trisubstituted double bond [1685 $cm^{-1}$ for (−)-**8** and (+)-**8**; 1689 $cm^{-1}$ for (+)-**9** and (−)-**9**]; (b) a tetrahydrofuran ring [$\delta_C$ 85.2, C-3a (see Scheme 1 for numbering) for (−)-**8** and (+)-**8**; $\delta_C$ 84.9, C-3a for (+)-**9** and (−)-**9**]; (c) a quaternary carbon linked to an oxygen and a nitrogen [$\delta_C$ 101.8, C-3′ for (−)-**8** and (+)-**8**; $\delta_C$ 101.5, C-3′ for (+)-**9** and (−)-**9**]; and (d) a $\gamma$-lactone conjugated with an exocyclic trisubstituted double bond [$\delta_C$ 168.2, C-1 and $\delta_H$ 6.9, H-7 for (−)-**8** and (+)-**8**; $\delta_C$ 168.0, C-1 and $\delta_H$ 6.98, H-7 for (+)-**9** and (−)-**9**] established the molecular connectivity of the stereoisomeric structures.

The 32 carbon and 39 hydrogen signals were assigned in the $^{13}C$ and $^{1}H$ NMR spectra (by DEPT, HMQC, HMBC, and NOESY experiments), confirming the proposed structures.[18]

Taking into account that *rac*-**3** possesses different electrophilic sites of varying reactivity toward nucleophiles, the mechanism explaining the formation of the lactam (Scheme 2) starts with a nucleophilic attack by the chiral amine on the carbonyl group of the enolic lactone (C-1′), formation of the ketone, and subsequent attack of the amide to the C-3′ carbonyl group via 5-*exo*-trigonal cyclization,[19] followed by a 1,4-Michael addition of the oxyanion to the C-3a/C-7a double bond, producing an ether bridge via a second 5-*exo*-trigonal cyclization. Subsequent tautomerization and protonation of the resultant enolate afford the products (Schemes 1 and 2).

The absolute configurations of compounds (−)-**8**, (+)-**8**, (+)-**9**, and (−)-**9** were established by analysis of the electronic CD curves using the exciton chirality method, which predicts that when two (or more) chromophores exhibiting strong $\pi \rightarrow \pi^*$ transitions have a chiral orientation of their interacting electric transition moments, the orientation between the chromophores will determine the sign of the Cotton effect.[20−22] The ECD curve of (−)-**8** (major product) exhibited


dx.doi.org/10.1021/np200645p | J. Nat. Prod. 2012, 75, 859−864

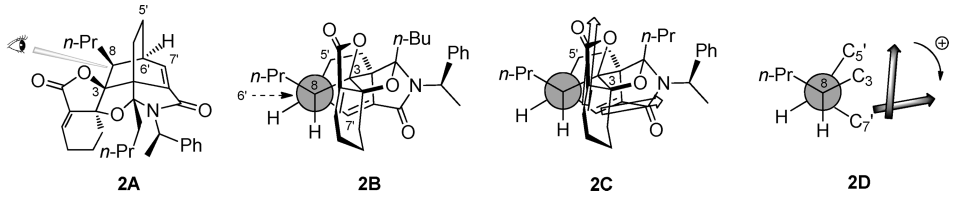


Figure 2.

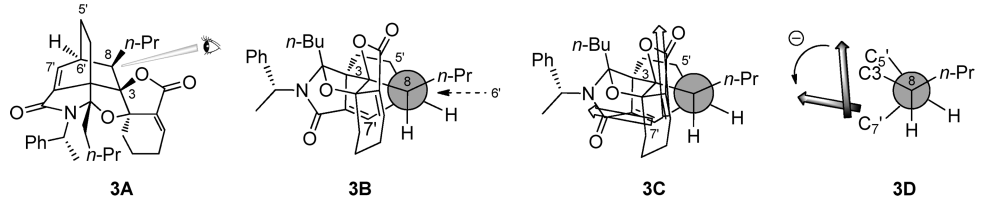


Figure 3.

a positive first Cotton effect at 246 nm ($\Delta\varepsilon$ +9.11) and a negative Cotton effect at 224 nm ($\Delta\varepsilon$ −20.29) due to exciton coupling between the $\alpha,\beta$-unsaturated $\gamma$-lactone and the $\alpha,\beta$-unsaturated $\gamma$-lactam chromophores, indicating that the transition dipole moments of the two chromophores were oriented in a clockwise manner. For illustrative purposes the Newman projection of the structure (Figure 2A) can be considered through the C-8/C-6′ $\sigma$ bond (Figure 2B), which clearly shows the clockwise orientation of the two chromophores defining a positive chirality (Figure 2C). This representation can be simplified as shown in Figure 2D, leading to assignment of the absolute configuration (3*S*, 3a*S*, 8*S*, 3′*R*, 3′a*S*, 6′*R*, 2″*R*) for compound 2A [structure (−)-**8**, Scheme 2].

(+)-**9** (shown in Figure 3A) displays a negative Cotton effect, which can be explained considering the Newman projections through the C-8/C-6′ $\sigma$ bond (Figure 3B and C). The arrangement of the chromophores determines a counterclockwise orientation of the electric transition moments [245 nm ($\Delta\varepsilon$ −7.89), 223 nm $\Delta\varepsilon$ +12.62] (Figures 3C and D), allowing the assignment of (3*R*, 3a*R*, 8*R*, 3′*S*, 3′a*R*, 6′*S*, 2″*R*) as its absolute configuration.

On the other hand, (+)-**8** and (−)-**9** showed Cotton effects of opposite signs compared with (−)-**8** and (+)-**9**: 245 nm ($\Delta\varepsilon$ −39.65), 224 nm ($\Delta\varepsilon$ +90.08) for the negative chirality, establishing the absolute configuration (3*R*, 3a*R*, 8*R*, 3′*S*, 3′a*R*, 6′*S*, 2″*S*) for (+)-**8**, and 245 nm ($\Delta\varepsilon$ +34.43), 223 nm ($\Delta\varepsilon$ −57.65) for the positive chirality, establishing the absolute configuration (3*S*, 3a*S*, 8*S*, 3′*R*, 3′a*S*, 6′*R*, 2″*S*) for (−)-**9**.

The absolute configurations proposed by the experimental data were confirmed by the calculated ECD curves of the optimized structures of (+)-**8** and (−)-**9** (see Supporting Information).

Following the computational details described in the Experimental Section, rotatory strengths were calculated for the velocity and length formalism,[23−25] and the computed data were used to reproduce the experimental ECD spectra. The two Cotton effects for both compounds (+)-**8** and (−)-**9** were in agreement with the experimental data (Figure 4). The computed ECD spectra of (+)-**8** and (−)-**9** exhibited the characteristic exciton-split CD curves due to the interaction of the electric transition moments of the $\alpha,\beta$-unsaturated $\gamma$-lactone and the $\alpha,\beta$-unsaturated $\gamma$-lactam chromophores. This exciton splitting could be attributed to the $\pi \rightarrow \pi^*$ transitions of the

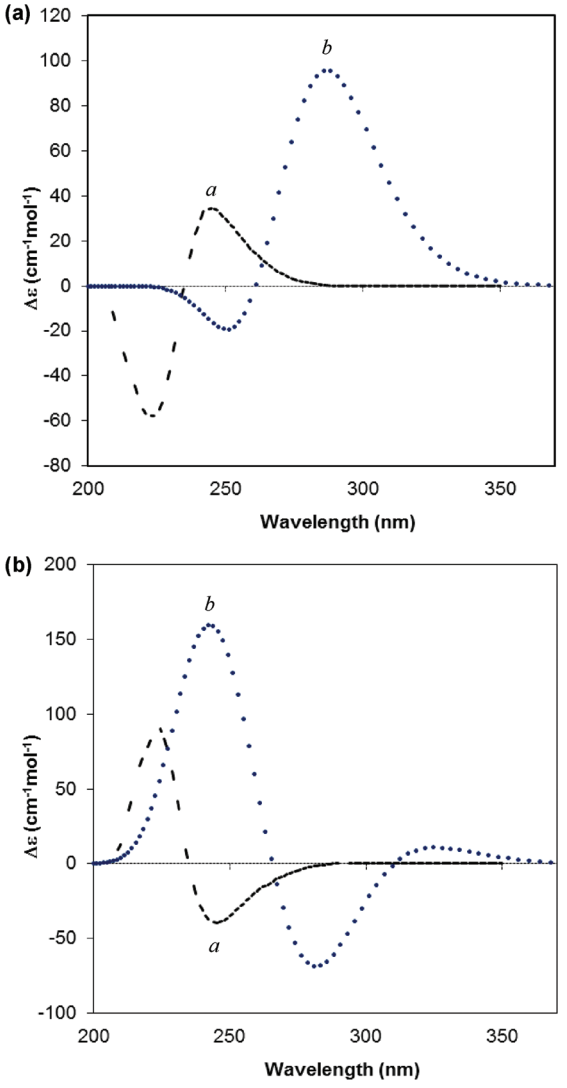


**Figure 4.** Comparison between the experimental (a, black --- line) and the theoretical ECD curves (b, blue ··· line) of (a) (+)-**8** and (b) (−)-**9**, respectively.

interacting electric transition moments of the chromophores of both molecules. The first positive Cotton effect and the negative Cotton effect of the theoretically computed ECD


dx.doi.org/10.1021/np200645p | *J. Nat. Prod.* 2012, 75, 859−864

spectra of (+)-**8** and (−)-**9**, respectively, were consequently in complete agreement with the experimental CD curves.

Encouraged by the previously reported biological activities of the natural phthalides, and taking into consideration their pharmacological importance,[16] it was decided to investigate the cytotoxic activity of these enantiomerically pure compounds toward three human cancer cell lines, following standard protocols.[26] The $IC_{50}$ values determined are shown in Table 1.

**Table 1. Evaluation of the $IC_{50}$ ($\mu$M) of the Natural Products and Derivatives of *L. porteri***

| compound | K562[a] | HCT-15[b] | SKLU-1[c] |
|---|---|---|---|
| *rac*-**3** | 26.6 ± 1.4 | 10.5 ± 0.9 | 7.1 ± 0.6 |
| *rac*-**5** | 46.1 ± 3.8 | 44.8 ± 1.3 | 13.2 ± 1.3 |
| (−)-**8** | 5.7 ± 0.9 | 5.4 ± 0.5 | 4.1 ± 0.1 |
| (+)-**9** | 21.7 ± 1.3 | 8.5 ± 0.6 | 5.9 ± 0.5 |
| (+)-**8** | 13.9 ± 1.6 | 7.5 ± 0.5 | 4.9 ± 0.3 |
| (−)-**9** | 5.2 ± 0.3 | 5.2 ± 0.2 | 4.3 ± 0.4 |
| helenalin[d] | 0.28 ± 0.02 | 0.29 ± 0.02 | 0.21 ± 0.02 |

[a]Leukaemia. [b]Colon. [c]Lung. [d]Positive control. Results are means ± SEM for three replicates.

The two pairs of enantiomers (−)-**8**/(+)-**8** and (+)-**9**/(−)-**9** were more potent compared with *rac*-**3** and *rac*-**5**, although less potent compared to the positive control (helenalin). Moreover, it was observed that compounds (−)-**8** and (−)-**9** were significantly more active than their enantiomers (+)-**8** and (+)-**9** in the cell lines K562 and HCT-15. This suggested that the compounds might have exerted their cytotoxic effect by interacting with a chiral target, and other derivatives of **8** and **9** would possibly shed light on this. For the SKLU-1 cell line only small differences between the enantiomers are noted.

The reaction between the racemic mixture of *rac*-**3** and (*R*)-(+)-$\alpha$-methylbenzylamine, as well as (*S*)-(−)-$\alpha$-methylbenzylamine, yielded two pairs of enantiomers, (±)-**8** and (±)-**9**, derived from the intramolecular cyclizations of the dimeric phthalides. The circular dichroism method and its rules together with the exciton chirality method were used to determine the absolute configuration of (−)-**8**, (+)-**8**, (−)-**9**, and (+)-**9**. The theoretical ECD curves of (+)-**8** and (−)-**9** were in agreement with the experimental spectra. The four enantiomers prepared were more potent toward the three human cancer cell lines compared to the natural products *rac*-**3** and *rac*-**5**, and (−)-**8** and (−)-**9** were, in general, more potent compared to their antipodes.

## EXPERIMENTAL SECTION

**General Experimental Procedures.** *rac*-Tokinolide B (*rac*-**3**) and *rac*-**5** were isolated from the acetone extract of the rhizomes of *L. porteri* by repeated column chromatography,[2] carried out on silica gel (230−400 mesh, Merck). Thin-layer chromatography analyses were done on aluminum-backed silica gel 60 F254 plates (0.20 mm thickness, Merck), and visualization of chromatograms was first done under a UV lamp and then with a solution of ammonium cerium sulfate, followed by drying and gentle heating. Infrared spectra were recorded with an FTIR Bruker TENSOR 27 instrument. Ultraviolet spectra were determined on a Shimadzu UV160U instrument. The optical rotation was measured in MeOH using a Perkin-Elmer 341 polarimeter. The $^1$H and $^{13}$C NMR experiments were performed at 25 °C using a Varian UnityPlus 500 spectrometer (at 500/125 MHz) and a Varian XR-300 (at 300/75 MHz); the spectra were recorded in $CDCl_3$, and the solvent residual signals (7.26 and 77.0 ppm for $^1$H and $^{13}$C NMR, respectively) were used as reference. The chemical shifts ($\delta$) are expressed in ppm relative to TMS, and the coupling constants ($J$) in Hz. EIMS and HRMS ($FAB^+$) spectra were recorded on a JEOL SX102A mass spectrometer, and the accurate mass was calculated using polyethylene glycol 400 as standard. The (*R*)-(+)- and (*S*)-(−)-$\alpha$-methylbenzylamine Chiraselect ≥99.0% (sum of enantiomers, GC) were purchased from Fluka Sigma-Aldrich.

**Derivatization of *rac*-Tokinolide B (*rac*-3) with (*R*)-(+)-$\alpha$-Methylbenzylamine.** To a solution of *rac*-tokinolide B (*rac*-**3**, 100.8 mg, 0.26 mmol) in anhydrous toluene (5 mL) placed in a stainless steel reactor (100 mL) was added (*R*)-(+)-$\alpha$-methylbenzylamine (0.06 mL, 57.12 mg, 0.47 mmol) under a nitrogen atmosphere. The reactor was sealed and heated (130 °C) for 20 h (pressure: 50 psi). After cooling to room temperature, the reaction mixture was concentrated at reduced pressure. EtOAc (10 mL) was added, and the organic phase was washed with HCl (10%), which subsequently was extracted with EtOAc (3 × 10 mL). The combined organic layer was washed with brine, dried with $Na_2SO_4$, and concentrated under reduced pressure. The residue was purified by column chromatography (*n*-hexane/EtOAc, gradient) to afford two products (76.6 mg, 70.2%):

(−)-**8** (44.6 mg, 40.9%) as a pale oil; $R_f$ 0.47 (*n*-hexane/EtOAc, 65:35); $[\alpha]^{25}_D$ −54.8 ($c$ 1.35 × $10^{-3}$, MeOH); UV (MeOH) $\lambda_{max}$ (log $\varepsilon$) 211 (4.4) nm; CD ($c$ 9.6 × $10^{-6}$, MeOH) 246 nm ($\Delta\varepsilon$ +9.11), 224 nm ($\Delta\varepsilon$ −20.29); IR ($CHCl_3$) $\nu_{max}$ 3349, 3061, 2959, 2872, 1766, 1689, 1494, 1454, 1351, 1214, 1166, 1037, 924, 752 $cm^{-1}$; $^1$H NMR ($CDC1_3$, 500 MHz; assignments by COSY, NOESY, and HMQC) $\delta$ 7.58 (2 H, dd, $J$ = 8.5, 1.5 Hz, H -4″, H-8″), 7.27 (2H, ddd, $J$ = 8.5, 7.5, 1.5 Hz, H-5″, H-7″), 7.20 (1H, dddd, $J$ = 8.5, 7.5, 1.5, 1.5, H-6″), 7.15 (1H, d, $J$ = 6.5 Hz, H-7′), 6.87 (1H, dd, $J$ = 7.0, 4.0 Hz, H-7), 4.85 (1H, q, $J$ = 7.0 Hz, H-2″), 2.90 (1H, dddd, $J$ = 10.5, 6.5, 4.0, 4.0 Hz, H-6′), 2.42 (1H, ddd, $J$ = 9.5, 7.0, 2.0 Hz, H-4′a), 2.20 (1H, dt, $J$ = 10.5, 4.5 Hz, H-6a), 1.98−1.92 (3H, m, H-6b, H-5′a, H-8′a), 1.90 (1H, d, $J$ = 7.5 Hz, H-9″), 1.76 (1H, ddd, $J$ = 9.5, 6.0, 6.0 Hz, H-8′b), 1.59 (1H, dd, $J$ = 10.5, 4.0, Hz, H-8), 1.45 (1H, dd, $J$ = 10.5, 4.0 Hz, H-4a), 1.35−1.32 (3H, m, H-5a, H-10a, H-5′b), 1.30−1.28 (1H, m, H-9a), 1.28−1.25 (4H, m, H-9′a, H-9′b, H-10′a, H-10′b), 1.19 (1H, ddd, $J$ = 11.5, 6.0, 6.0 Hz, H-4′b), 1.12−1.05 (2H, m, H-5b, H-10b), 0.99 (1H, dd, $J$ = 10.0, 4.0 Hz, H-9b), 0.90 (1H, ddd, $J$ = 10.0, 6.0, 6.0 Hz, H-4b), 0.86 (3H, t, $J$ = 7.0 Hz, $CH_3$-11), 0.83 (3 H, t, $J$ = 7.5 Hz, $CH_3$-11′); $^{13}$C NMR ($CDCl_3$, 125 MHz, assignments by DEPT, HSQC, and HMBC) $\delta$ 168.2 (CO, C-1), 165.2 (CO, C-1′), 143.4 (C, C-3″), 140.2 (CH, C-7), 139.2 (C, C-7′a), 137.4 (CH, C-7′), 130.8 (C, C-7a), 128.2 (CH, C-5″, C-7″), 128.0 (CH, C-4″, C-8″), 127.1 (CH, C-6″), 101.8 (C, C-3′), 95.3 (C, C-3), 85.2 (C, C-3a), 57.0 (C, C-3′a), 52.7 (CH, C-2″), 45.5 (CH, C-8), 36.2 (CH, C-6′), 35.0 ($CH_2$, C-8′), 29.0 ($CH_2$, C-4), 28.8 ($CH_2$, C-9), 25.7 ($CH_2$, C-9′), 25.0 ($CH_2$, C-6), 23.9 ($CH_2$, C-4′), 23.0 ($CH_2$, C-10′), 20.9 ($CH_2$, C-10), 19.5 ($CH_3$, C-9″), 17.4 ($CH_2$, C-5′), 16.8 ($CH_2$, C-5), 14.1 ($CH_3$, C-11), 13.7 ($CH_3$, C-11′); EIMS $m/z$ 501 $[M]^+$ (15), 378 (17), 310 (8), 274 (33), 191 (100), 149 (10), 120 (32), 105 (28), 55 (5); HRMS ($FAB^+$) $m/z$ 502.2959 (calcd for $C_{32}H_{39}O_4N+H^+$ 502.2957).

(+)-**9** (31.9 mg, 29.3%) as a pale oil; $R_f$ 0.44 (*n*-hexane/EtOAc, 65:35); $[\alpha]^{25}_D$ +7.8 ($c$ 1.15 × $10^{-3}$, MeOH); UV (MeOH) $\lambda_{max}$ (log $\varepsilon$) 210 (4.5) nm; CD ($c$ 7.2 × $10^{-6}$, MeOH) 245 ($\Delta\varepsilon$ −7.89), 223 ($\Delta\varepsilon$ +12.62); IR ($CHCl_3$) $\nu_{max}$ 3347, 3060, 2958, 2872, 1765, 1688, 1526, 1495, 1452, 1352, 1214, 1036, 1013, 924, 751 $cm^{-1}$; $^1$H NMR ($CDC1_3$, 500 MHz; assignments by COSY, NOESY, and HMQC) $\delta$ 7.47 (2H, dd, $J$ = 7.5, 1.5 Hz, H-4″, H-8″), 7.29 (2H, ddd, $J$ = 7.5, 7.5, 1.5 Hz, H-5″, H-7″), 7.22 (1H, dddd, $J$ = 7.5, 7.5, 1.5, 1.5, H-6″), 7.22 (1H, d, $J$ = 6.5 Hz, H-7′), 6.98 (1H, dd, $J$ = 7.0, 4.0 Hz, H-7), 4.69 (1H, q, $J$ = 7.0 Hz, H-2″), 2.93 (1H, dddd, $J$ = 10.0, 6.5, 4.0, 4.0 Hz, H-6′), 2.46−2.39 (2H, ddd, $J$ = 11.0, 4.0, 4.0 Hz, H-6a, H-4′a), 2.19−2.16 (1H, m, H-6b), 1.99−1.89 (3H, m, H-5a, H-5′a, H-8′a), 1.85 (3H, d, $J$ = 7.0 Hz, H-9″), 1.63 (1H, ddd, $J$ = 11.0, 4.5, 4.5 Hz, H-8′b), 1.65 (1H, ddd, $J$ = 10.0, 3.0, 3.0 Hz, H-8), 1.51 (1H, ddd, $J$ = 10.0, 4.5, 4.5 Hz, H-4a), 1.37−1.33 (3H, m, H-5b, H-10a, H-5′b), 1.73 (1H, dt, $J$ = 6.5, 3.0, H-9a), 1.28−1.25 (1H, m, H-9b), 1.23−1.17 (2H, m, H-10b, H-4′b), 1.15−1.09 (2H, m, H-9′a, H-10′a), 1.02−0.96 (3H, m, H-4b, H-9′b, H-10′b), 0.87 (3H, t, $J$ = 7.0 Hz, $CH_3$-11), 0.66 (3H, t, $J$ = 7.0 Hz, $CH_3$-11′); $^{13}$C NMR ($CDCl_3$, 125 MHz, assignments by DEPT, HSQC, and HMBC) $\delta$ 168.0 (CO, C-1), 165.0 (CO, C-1′), 143.2 (C,


dx.doi.org/10.1021/np200645p | J. Nat. Prod. 2012, 75, 859−864

C-3″), 140.0 (CH, C-7), 139.6 (C, C-7′a), 137.4 (CH, C-7′), 130.8 (C, C-7a), 128.4 (CH, C-5″, C-7″), 127.0 (CH, C-4″, C-8″), 126.9 (CH, C-6″), 101.5 (C, C-3′), 95.7 (C, C-3), 84.9 (C, C-3a), 56.9 (C, C-3′a), 54.1 (CH, C-2″), 45.4 (CH, C-8), 36.3 (CH, C-6′), 34.8 ($CH_2$, C-8′), 29.0 ($CH_2$, C-4), 28.8 ($CH_2$, C-9), 25.7 ($CH_2$, C-9′), 25.1 ($CH_2$, C-6), 24.0 ($CH_2$, C-4′), 22.8 ($CH_2$, C-10′), 21.0 ($CH_2$, C-10), 20.3 ($CH_3$, C-9″), 17.6 ($CH_2$, C-5′), 17.3 ($CH_2$, C-5), 14.1 ($CH_3$, C-11′), 13.6 ($CH_3$, C-11); EIMS *m/z* 501 $[M]^+$ (24), 378 (60), 310 (16), 274 (86), 228 (10), 191 (100), 149 (18), 120 (38), 105 (58), 79 (8), 55 (7); HRMS ($FAB^+$) *m/z* 502.2961 (calcd for $C_{32}H_{39}O_4N+H^+$ 502.2957).

**Derivatization of *rac*-Tokinolide B (*rac*-3) with (*S*)-(−)-α-Methylbenzylamine.** To a solution of *rac*-tokinolide B (*rac*-**3**, 250 mg, 0.65 mmol) in dry toluene (5 mL) placed in a stainless steel reactor (100 mL) was added (*S*)-(−)-α-methylbenzylamine (0.16 mL, 152.3 mg, 1.25 mmol) under a nitrogen atmosphere. The reactor was sealed and heated (130 °C) for 20 h (pressure: 50 psi). After cooling to room temperature, the reaction mixture was concentrated at reduced pressure. EtOAc (10 mL) was added, and the organic phase was washed with HCl (10%), which subsequently was extracted with EtOAc (3 × 10 mL). The combined organic layer was washed with brine, dried with $Na_2SO_4$, and concentrated under reduced pressure. The residue was purified by column chromatography (*n*-hexane/EtOAc, gradient), affording (234 mg, 71%) two pure products. The NMR data were identical to their enantiomers.

(+)-**8** (96.24 mg, 29.2%) as a pale oil; $[\alpha]^{25}_D$ +46.2 (*c* 1.30 × $10^{-3}$, MeOH); UV (MeOH) $\lambda_{max}$ (log ε) 217 nm (4.3); CD (*c* 4.0 × $10^{-6}$, MeOH) 245.5 nm (Δε −39.65), 224.5 nm (Δε +90.08); HRMS ($FAB^+$) *m/z* 502.2964 (calcd for $C_{32}H_{39}O_4N+H^+$ 502.2959).

(−)-**9** (137.8 mg, 41.8%) as a pale oil; $[\alpha]^{25}_D$ −8.12 (*c* 1.60 × $10^{-3}$, MeOH); UV (MeOH) $\lambda_{max}$ 216 nm (4.3); CD (*c* 4.4 × $10^{-6}$, MeOH) 245 nm (Δε +34.43), 223 nm (Δε −57.65); HRMS ($FAB^+$) *m/z* 502.2964 (calcd for $C_{32}H_{39}O_4N+H^+$ 502.2957).

**Cytotoxicity Assay.** Colon (HCT-15), leukemia (K-562), and lung (SKLU-1) human tumor cell lines were supplied by National Cancer Institute (NCI), USA. The cytotoxicity of the test compounds was determined using the protein-binding dye sulforhodamine B (SRB) in microculture assay to measure cell growth.[26] The cell lines were cultured in RPMI-1640 (Sigma Chemical Co., Ltd., St. Louis, MO, USA), supplemented with 10% fetal bovine serum, 2 μM L-glutamine, 100 IU/mL penicillin G, 100 μg/mL streptomycin sulfate, and 0.25 μg/mL amphotericin B (Gibco). They were maintained at 37 °C in a 5% $CO_2$ atmosphere with 95% humidity. For the assay, 5 × $10^4$ cell/mL (K562), 10 × $10^4$ cell/well (HCT-15), 7500 cell/mL (SKLU-1), and 100 μL/well of these cell suspensions were seeded in 96-well microtiter plates and incubated to allow the cell attachment. After 24 h, 100 μL of each test compound and positive control was added to the wells. After 48 h, adherent cell cultures were fixed in situ by adding 50 μL of cold 50% (w/v) trichloroacetic acid (TCA) and incubated for 60 min at 4 °C. The supernatant was discarded, and the plates were washed three times with $H_2O$ and air-dried. Cultures fixed with TCA were stained for 30 min with 100 μL of 0.4% SRB solution. Protein-bound dye was extracted with 10 μM unbuffered Tris base, and the optical densities were read on an Ultra microplate reader (Elx 808, BIO-TEK Instruments, Inc.), with a test wavelength of 515 nm. Results were expressed as inhibitory concentration 50 values, they were calculated according to the protocol of Monks,[26] where a dose−response curve was plotted for each compound, and the concentration giving 50% inhibition ($IC_{50}$) was estimated from linear regression equations. The $IC_{50}$ values (mean ± standard error for three replicates) are shown in Table 1.

**Computational Details.** To obtain minimum energy conformations for structures (+)-**8** and (−)-**9**, we followed a geometry optimization (GO) by consecutive addition of a molecular fragment at the time. For this purpose a basic central molecular fragment was modeled. This fragment was submitted to a geometry optimization computation with AM124 followed by a subsequent density functional GO, with the hybrid functional B3LYP using the 6-311G** basis set.[24] A new molecular fragment was modeled on the previously optimized one, and a new GO with AM1 and B3LYP was carried out. This paradigm was followed until the full molecular structure was completed. Once (+)-**8** and (−)-**9** were completed and optimized, an ECD calculation was carried out within the time-dependent density functional theory formalism, using the B3LYP functional with the 6-311G** basis set previously employed. All the described molecular modeling was done with GaussView,[23] whereas the described quantum mechanical computations were carried out with the suite of programs in Gaussian 03.[24]

The ECD spectrum was simulated by overlapping Gaussian functions for each transition according to

$$\Delta\varepsilon(E) = \left(\frac{1}{2.297^{-39}}\right)\left(\frac{1}{\sqrt{2\pi\sigma}}\right)\sum_{\alpha}(\Delta E_{0a})(R_{0a})\exp\left[-\left(\frac{(E-\Delta E_{0a})}{2\sigma}\right)^2\right]$$

where σ is the width of the band at 1/*e* height and $\Delta E_{0a}$ and $R_{0a}$ are the excitation energies and rotatory strengths. A σ value of 0.2 eV was used.[25]

## ■ ASSOCIATED CONTENT

### Ⓢ Supporting Information

NMR spectra for compounds (−)-**8**, (+)-**8**, (+)-**9**, and (−)-**9**, and figures depicting the minimum energy structures of (+)-**8** and (−)-**9** obtained by computational methods. This material is available free of charge via the Internet at http://pubs.acs.org.

## ■ AUTHOR INFORMATION


### Corresponding Author

*Tel: +52 (55) 5622-4446. Fax: +52 (55) 5616-2217. E-mail: delgado@unam.mx.


### Notes

The authors declare no competing financial interest.

## ■ ACKNOWLEDGMENTS


Financial support from CONACyT (scholarship 181999, project 102158), DGEP-UNAM, and ALFA-project AML/B7-311/97/0666/II-0375-FA (Sweden) is gratefully acknowledged. J.A.C. is grateful to DGSCA-UNAM for the generous allocation of CPU time. We thank M. I. Chávez, B. Quiroz-García, M. T. Ramírez-Apan, E. García, R. Patiño, J. Pérez-Flores, L. Velasco, and D. Vázquez for technical assistance. This work was taken in part from the Ph.D. thesis of A.L.


## ■ REFERENCES


(1) León, A.; Toscano, R. A.; Tortoriello, J.; Delgado, G. *Nat. Prod. Res.* **2011**, *25*, 1234−1242.

(2) Delgado, G.; Reza-Garduño, R. G.; Toscano, R. A.; Bye, R.; Linares, E. *Heterocycles* **1988**, *27*, 1305−1312.

(3) Quiroz-García, B.; Hernández-Ortega, S.; Sterner, O.; Delgado, G. *Tetrahedron* **2004**, *60*, 3681−3688.

(4) Quiroz-García, B.; Figueroa, R.; Cogordán, J. A.; Delgado, G. *Tetrahedron Lett.* **2005**, *46*, 3003−3006.

(5) Rios, M. Y.; Delgado, G.; Toscano, R. A. *Tetrahedron* **1998**, *54*, 3355−3366.

(6) Ogawa, Y.; Mori, Y.; Maruno, M.; Wakamatsu, T. *Heterocycles* **1997**, *45*, 1869−1872.

(7) Rios, M. Y.; Delgado, G. *Rev. Soc. Quím. Méx.* **1999**, *43*, 127−132.

(8) Beck, J. J.; Stermitz, F. R. *J. Nat. Prod.* **1995**, *58*, 1047−1055.

(9) Quiroz-García, B.; Hernández, L.; Toscano, R. A.; Sterner, O.; Delgado, G. *Tetrahedron Lett.* **2003**, *44*, 2509−2512.

(10) Linares, E.; Bye, R. A. *J. Ethnopharmacol.* **1987**, *19*, 153−183.

(11) Bye, R. A. *Econ. Bot.* **1986**, *40*, 103−124.

(12) Teng, C.-M.; Chen, W.-Y.; Ko, W.-C.; Ouyang, C. *Biochim. Biophys. Acta* **1987**, *924*, 373−382.

(13) Ko, W.-C.; Sheu, J.-R.; Tzeng, S.-H.; Chen, C.-M. *Planta Med.* **1998**, *64*, 229−232.

(14) Ko, W. C.; Liao, C.-C.; Shih, C.-H.; Lei, C.-B.; Chen, C.-M. *Planta Med.* **2002**, *68*, 1004−1009.
(15) Lin, G.; Chan, S. S. K.; Chung, H. S.; Li, S. L. In *Studies in Natural Products Chemistry*; Atta-ur-Rahman, Ed.; Elsevier: Amsterdam, 2006; Vol. *32*, Bioactive Natural Products Part L, pp 611−669.
(16) Beck, J. J.; Chou, S. J. *J. Nat. Prod.* **2007**, *70*, 891−900.
(17) García, A.; Ramírez-Apan, T.; Cogordán, J. A.; Delgado, G. *Can. J. Chem.* **2006**, *84*, 1593−1602.
(18) It is interesting to note that in the $^1$H NMR spectra of compounds (+)-**9** and (−)-**9** the methyl group $CH_3$-11′ is shielded [$\delta_H$ 0.66 (3H, t, $J$ = 7 Hz)] presumably due to the alignment of this group above the benzene moiety (in agreement with the calculated structure (−)-**9**; see Supporting Information). For the methyl protons $CH_3$-11′ of the enantiomers (−)-**8** and (+)-**8** this effect was not observed [$\delta_H$ 0.86 (3H, t, $J$ = 7 Hz)].
(19) Baldwin, J. E.; Lusch, M. J. *Tetrahedron* **1982**, *38*, 2939−2947.
(20) Harada, N.; Nakanishi, K. *Acc. Chem. Res.* **1972**, *5*, 257−263.
(21) Harada, N.; Nakanishi, K. *Circular Dichroic Spectroscopy-Exciton Coupling in Organic Stereochemistry*; University Science Books, Mill Valley, CA, and Oxford University Press, Oxford, 1983.
(22) Berova, N.; Di Bari, L.; Pescitelli, G. *Chem. Soc. Rev.* **2007**, *36*, 914−931.
(23) Dennington, R., II; Keith, T.; Millam, J. *GaussView*, Version 4.1; Semichem, Inc.,: Shawnee Mission, KS, 2007.
(24) Frisch, M. J.; Trucks, G. W.; Schlegel, H. B.; Scuseria, G. E.; Robb, M. A.; Cheeseman, J. R., Montgomery, J. A.; Vreven, T.; Kudin, K. N.; Burant, J. C.; Millam, J. M.; Lyengar, S. S.; Tomasi, J.; Barone, V.; Mennucci, B.; Cossi, M.; Scalmani, G.; Rega, N.; Petersson, G. A.; Nakatsuji, H.; Hada, M.; Ehara, M.; Toyota, K.; Fukuda, R.; Hasegawa, J.; Ishida, M.; Nakajima, T.; Honda, Y.; Kitao, O.; Nakai, H.; Klene, M.; Li, X.; Knox, J. E.; Hratchian, H. P.; Cross, J. B.; Adamo, C.; Jaramillo, J.; Gomperts, R.; Stratmann, R. E.; Yazyev, O.; Stratmann, R. E.; Austin, A. J.; Cammi, R.; Pomelli, C.; Ochterski, J.; Ayala, P. Y.; Morokuma, K.; Voht, G. A.; Salvador, P.; Dannenberg, J. J.; Zakrzewski, V. G.; Dapprich, S.; Daniels, A. D.; Strain, M. C.; Farkas, O.; Malick, D. K.; Rabuck, A. D.; Raghavachari, K.; Raghavachari, K.; Foresman, J. B.; Ortiz, J. V.; Cui, Q.; Baboul, A. G.; Clifford, S.; Cioslowski, J.; Stefanov, B. B.; Liu, G.; Liashenko, A.; Piskorz, P.; Komaromi, I.; Martin, R. L.; Fox, D. J.; Keith, T.; Al-Laham, M. A.; Peng, C. Y.; Nanayakkara, A.; Challacombe, M.; Gill, P. M. W.; Johnson, B. G.; Chen, W.; Wong, M. W.; Gonzalez, C.; Pople, J. A. *Gaussian 03*, Revision B.05; Gaussian, Inc.: Pittsburgh, PA, 2003.
(25) Diedrich, C.; Grimme, S. *J. Phys. Chem. A* **2003**, *107*, 2524−2539.
(26) Monks, A.; Scudiero, D.; Skehan, P.; Shoemaker, R.; Paull, K.; Vistica, D.; Hose, C.; Langley, J.; Cronise, P.; Vaigro-Wolff, A.; Gray-Goodrich, M.; Campbell, H.; Mayo, J.; Boyd, M. *J. Natl. Cancer Inst.* **1991**, *83*, 757−766.